LIMNOLOGY
and
OCEANOGRAPHY

ASLO

Limnol. Oceanogr. 63, 2018, 1191–1203

doi: 10.1002/lno.10764

Increased nutrients from aeolian-dust and riverine origin decrease the CO_2-sink capacity of coastal South Atlantic waters under UVR exposure

Marco J. Cabrerizo [1,2,3]* **Presentación Carrillo,** [2,3] **Virginia E. Villafañe,** [1,4] **Juan Manuel Medina-Sánchez** [2] **E. Walter Helbling** [1,4]

[1]Estación de Fotobiología Playa Unión, Rawson, Chubut, Argentina
[2]Facultad de Ciencias, Departamento de Ecología, Universidad de Granada, Granada, España
[3]Instituto Universitario de Investigación del Agua, Universidad de Granada, Granada, España
[4]Consejo Nacional de Investigaciones Científicas y Técnicas (CONICET), Buenos Aires, Argentina

Abstract

Increases in ultraviolet radiation (UVR) levels due to the ongoing stratification of water bodies and higher nutrient concentrations either through riverine or aeolian-dust-inputs are expected in the near future in coastal surface waters. Here, we combined remote-sensing data of particulate organic carbon (POC; 1997–2016 period), observational data of solar radiation (1999–2015 period), and a mid-term experimental approach with coastal plankton communities from South Atlantic Ocean (SAO) to test how the interaction between increased nutrients by riverine and aeolian-dust inputs and high UVR may alter the community dynamics and the CO_2 sink capacity of these ecosystems in the future. Our results show a decline ~ 27% in the sink capacity of the coastal ecosystems regardless of the nutrient source considered and under high UVR levels. This decreased CO_2 uptake was coupled with a high dynamic photoinhibition and dark recovery of photosystem II and shifts in the community structure toward the dominance by nano-flagellates. Moreover, remote-sensing data also evidences an incipient tipping point with decreasing POC values in this area over the annual planktonic succession. Therefore, we propose that to continue this climate and human-mediated pressure, these metabolic responses could be strengthened and extended to other productive coastal areas.

The growth of the human population and activities (e.g., agriculture, herding, deforestation, industries) causes a substantial transfer of nutrients, mainly nitrogen (N) and phosphorus (P) to adjacent freshwater bodies, followed by their transport to coastal waters (Peñuelas et al. 2013). Together with these massive human-caused additions, climate variability due to global change (i.e., more severe droughts, storms, and alterations in wind patterns) is also causing increases in the atmospheric N and P deposition into coastal areas (Mahowald et al. 2008). As a result of these perturbations, coastal habitats are currently confronted with several alterations (i.e., hypoxia, reduced water transparency) which are triggering cascade effects on the ecosystem functioning (i.e., less suitable habitats for feeding and reproduction, more harmful phytoplankton blooms) (Harding et al. 2016; Maar et al. 2016). In addition to changes in nutrient concentrations, solar radiation in the water column is being greatly altered by global change. Due to global warming, stratification of the water bodies tends to increase and, therefore, organisms are expected to receive higher solar radiation levels (particularly the ultraviolet radiation portion, UVR, 280–400 nm) than at present (Williamson et al. 2014).

Previous studies conducted with planktonic communities have shown a stimulatory individual effect of nutrient inputs linked or not to aeolian dust, increasing the PSII performance (Φ_{PSII}) (Browning et al. 2014), primary production (PP) (Marcoval et al. 2008; Ridame et al. 2014), bacterial growth (Lekunberri et al. 2010; Teira et al. 2016), and respiration (Medina-Sánchez et al. 2017). Conversely, other studies have also found inhibitory effects of these inputs on the aforementioned processes, due to the presence of toxic elements (e.g., Cu, Pb) (Hoffmann et al. 2012; Dao and Beardall 2016). Also, recent studies have shown that nutrients can trigger abrupt changes in community structure toward dominance by only one functional group (e.g., fast-growing diatoms) (Macías et al. 2010; Villafañe et al. 2017). This can promote greater heterotrophy by increased community respiration (Martínez-García et al. 2013), thus altering the energy transfer to higher trophic levels (Tsagaraki et al. 2017). On the other hand, it is known that current or enhanced levels

*Correspondence: mjc@ugr.es

Additional Supporting Information may be found in the online version of this article.

of UVR inhibits the PP (Helbling et al. 2015; Villafañe et al. 2015), nutrient uptake (Hessen et al. 2012), Φ_{PSII} or DNA repair (Jeffrey et al. 2000; Harrison et al. 2015; Villafañe et al. 2017); however, although the combined impact of both global change drivers is generally considered antagonistic (e.g., nutrients attenuate the harmful effect of UVR), recent results by Carrillo et al. (2015) and Harrison et al. (2015) evidence that nutrient inputs can also unmask the harmful UVR effects on planktonic responses.

Thus, because inorganic nutrients and solar radiation are pivotal for the functioning of the global C-cycle, one of the unresolved issues in global-change research is whether rising nutrient availability, due either to riverine or aeolian-dust inputs, and high UVR fluxes could impact the carbon uptake by primary producers and the total respiration by the planktonic community. Therefore, if both processes are unbalanced in a scenario of global change, the capacity of any ecosystem as CO_2-sink of the human-induced carbon dioxide (CO_2) emissions could be greatly altered in the future. This would be especially relevant for the Southwest Atlantic Ocean (SAO), which not only is one of the most productive regions worldwide, with rich and diverse communities (Acha et al. 2004; Romero et al. 2006), but is also considered one of the most intense CO_2 sinks per unit area in the global Ocean (Bianchi et al. 2009).

To shed new light on how the metabolic functioning of coastal areas may be impacted by the ongoing environmental change, we developed a dual approach: (1) a 20-yr observational study with remote-sensing and field data through which we evaluate long-term trends in the frequency and intensity of aeolian-dust deposition (and riverine inputs) and solar radiation on SAO, and how it could be altering the production of particulate organic carbon over the seasonal phytoplankton succession; and (2) a mid-term manipulation study where we experimentally increased the nutrient concentrations, mimicking future aeolian-dust deposition and riverine inputs, under high UVR exposure to determine their effects on photosynthetic activity and metabolic responses as well as on the structure of a microplanktonic community from Patagonian coastal waters. We used this area as model ecosystem to measure variations in the net primary production (NPP), daily community respiration (CR), and gross primary production (GPP) at short- and mid-term scales. From these data, we quantified how both global-change scenarios considered could alter the capacity of SAO coastal waters to sequester atmospheric CO_2.

Methods

Model ecosystem

The Chubut River estuary, together with its area of influence, is a meso-tidal and highly productive estuary in Patagonia (Piccolo and Perillo 1999) characterized by a variable range of physical (kd_{PAR} ranging $\sim$ 1–6 m^{-1}), chemical (N, P, and silicate [Si] concentrations [*see* "Experimental set up"]), and biological (characteristic seasonal succession with a pre-bloom, bloom, and post-bloom period) conditions due to the interaction between the SAO and the mouth of Chubut River (Helbling et al. 2010). The study area has intense horticultural production, animal-breeding farms, and different cities ($\sim$ 140.000 inhabitants in total; Censo Nacional de Población, Hogares y Viviendas, 2010; INDEC - DGEyC) located along the riverbanks in the last 100 km before reaching the sea. All this implies a continuous supply of nutrients to this marine area. Also, this ecosystem is characterized by high-speed ($\sim$ 25 m s^{-1}) and frequent (10^4 min) southwestern winds throughout the year except in winter, where they are minimum ($\sim$ 3.5–4.5 m s^{-1}) (Helbling et al. 2005). Due to these intense and frequent winds, Patagonia is currently considered one of the high-latitude areas (> 50°N and > 40°S) most active in terms of aeolian-dust deposition, particularly during the spring (October–November) and late summer (March–April), which provide nutrients (mainly P and N) to the surrounding marine system (Bullard et al. 2016). Additionally, the high wind speeds registered in this area cause a constant mixing of the water column in surface layers, and thus organisms undergo highly variable light at short and mid-term scales over the year (Helbling et al. 2005).

Sampling and experimental set up

Surface seawater (0.5 m depth and salinity > 33) was collected at the mouth of the Chubut River estuary (Egi station, 43° 18.8′S, 65° 02.0′W) during high tide on the afternoon of 19th October 2014 using an acid-cleaned (1N HCl) bucket. The sample (200 L in total) was pre-screened through a 180 μm Nitex mesh to eliminate mesozooplankton, placed in 25-L opaque acid-washed containers and transported immediately to the EFPU (10–15 min away from the sampling site) where the experiment was set as follows: the set-up consisted on 18 microcosms (10L-UVR-transparent bags, Alpax Trade Lab, São Paulo, Brazil, 72% transmission at 280 nm) where seawater samples were held. A 2 × 3 factorial design (in triplicate) was implemented with: (a) Two solar radiation treatments, (1) PAB (PAR + UV-A + UV-B, > 280 nm; uncovered microcosms), and (2) P (PAR > 400 nm; microcosms covered with Ultraphan 395 nm filter); and (b) three nutrient treatments, (1) ambient (amb), where non-manipulated nutrient concentrations were nitrite + nitrate (N) = 2.4 μM, phosphate (P) = 1.76 μM and silicate (Si) = 1.7 μM, (2) riverine inputs (riv) through the addition of inorganic nutrients, i.e., $NaNO_3$, NaH_2PO_4, and Na_2SiO_3 as majority sources of N, P, and Si, respectively, which increased the nutrient concentrations with respect to ambient conditions in 61.98 μM (N), 30.84 μM (P), and 135.37 μM (Si), and (3) aeolian-dust inputs, whose addition increased the nutrient concentrations in 0.31 μM (N), 1.15 μM (P), and 4.90 μM (Si).

The experimental addition of inorganic nutrients used in this study simulated increases of ca. 8 and ca. sixfold for N and P, respectively, with respect to the historic maximal concentrations (1986–2013) registered in the study area over an annual cycle (2–8 μM and 2–5 μM for N and P, respectively; *see* Bermejo et al. 2018 for a detailed analysis). Si concentrations, however, were in the mean range of those received over the year as their concentrations had remained stable over the last three decades (100–200 μM; Bermejo et al. 2018). The dust added (size ranging between 1–10 μm) was collected in situ in Merzouga (Tafilalet, Morocco, 31° 6′.00 N, 3° 59′.24 W) and fractioned as described in Cabrerizo et al. (2016). Thus, the dust was broadly comparable with that used in previous reports showing that those particles larger than this size are rapidly removed during the atmospheric transport (Guieu et al. 2010). The rationale behind adding a single pulse of Saharan dust as a model continental dust source lies in the fact that: (1) the Sahara desert is responsible for 58% of the global dust emissions each year (Tanaka and Chiba 2006), and (2) these kinds of atmospheric inputs are significantly increasing the N and P concentrations in aquatic ecosystems, particularly in the Southern Hemisphere (Brahney et al. 2015).

The amount of dust added in the experiment (4.1 mg L^{-1}) simulates a deposition scenario of 61.5 mg m^{-2} into a 15-m-deep water layer, which constitutes the water layer potentially affected after intense dust-deposition events (Pulido-Villena et al. 2008; Marañón et al. 2010). Therefore, if we consider that: (1) the mean number of dust-deposition events per year in the area during the last two decades $\sim$ 100, (2) the annual dust-deposition rates on South Atlantic Ocean is $\sim$ 500 mg m^{-2} yr^{-1} (Jickells and Moore 2015) and (3) that most of aeolian-dust deposition occurs in single and strong pulses (Guerzoni et al. 1997), we simulate a future scenario of increases of up to 12-fold in dust inputs through a single deposition event.

All microcosms were placed in 200-L tanks with running water to maintain the in situ temperature (14.5°C) and exposed to natural solar radiation for 5 d. The thin water layer ($\sim$ 0.5 m) that covered the microcosms simulated an extreme scenario with a shallow upper mixed layer (UML). The microcosms were shaken manually several times a day so that plankton received homogeneous irradiance during the exposure by preventing organisms from settling to the bottom.

Sub-samples for different measurements/analyses were taken daily [for chlorophyll *a* (Chl *a*) determinations, oxygen (O_2) concentration, and effective photochemical quantum yield (Φ_{PSII}) measurements and for changes in the picoplanktonic fraction] or every other day (taxonomic composition of nanoplanktonic fraction and nutrient analyses) using a syringe attached to a silicone tube inserted into each microcosm to prevent their tampering.

Measurements and analyses

Long-term remote-sensing and observational data

Data from the daily aerosol index (AI) and monthly particulate organic carbon (POC) for the Egi station were downloaded from Giovanni v 4. 18. 3 Earth database of the National Aeronautics and Space Administration (NASA) (Acker and Leptoukh 2007). For the period 1996–2015, AI data were provided by the Total Ozone Mapping Spectrometer-Earth Probe (TOMS-EP) (22 July 1996 to 31 December 2003) and by the Ozone Monitoring Instrument (OMI) (01 January 2004 to 31 December 2015) satellites, respectively. As previous studies (Bullejos et al. 2010; Cabrerizo et al. 2016) established that an AI > 0.5 constitutes a deposition event, we also considered the annual dust deposition events as the number of days per year affected by events of AI > 0.5. For monthly POC, data were provided by sea-viewing wide field-of-view sensor (SeaWiFS, 04 September 1997 to 31 December 2010) and by moderate-resolution imaging spectroradiometer (MODIS, 01 January 2011 to 31 October 2016).

Solar-radiation measurements: long-term and experimental data

We monitored the incident solar radiation during the experiments using an ELDONET (Real Time Computers, Germany) broadband-filter radiometer that measures UV-B, UV-A, and PAR (400–700 nm) every second, averages the data over a 1-min interval, and stores them in a computer. The radiometer is routinely calibrated (once a year) using a solar calibration procedure. For this calibration, the irradiance data during clear-sky conditions are compared with the output of models for transfer of atmospheric radiation (Björn and Murphy 1985). Also, daily PAR doses over the study area for the 1999–2015 period were taken from the Estación de Fotobiología Playa Unión (EFPU) online database (*see* http://www.efpu.org.ar).

Chl *a* measurements

Water samples (100 mL) to determine Chl *a* concentration were taken from each microcosm every day early in the morning and filtered onto M-GF (25 mm) filters (Muntkell, Sweden). Afterwards, photosynthetic pigments were extracted in absolute methanol as described in Holm-Hansen and Riemann (1978) and a scan between 250 nm and 750 nm using a spectrophotometer (Hewlett Packard, model HP 8453E). Chl *a* concentrations were calculated using the equations of Porra (2002).

Nutrient analyses

Samples from each microcosm were placed in 125 mL HDPE bottles and frozen (–20°C) until analyses, to determine nitrogen, phosphorus, and silicate concentrations using spectrophotometric techniques, as described in Strickland and Parsons (1972).

Taxonomic analyses

Samples for the identification and/or counting of autotrophic nanoplankton (ANP) under inverted microscope were taken at the first and at the last day of exposure to solar radiation, whereas

samples for autotrophic picoplankton (APP) and heterotrophic picoplankton (HPP) counting through flow cytometry were taken on a daily basis due to their high division rates. For ANP, samples were placed in 125 mL brown glass bottles and fixed with buffered formalin (final concentration 0.4% of formaldehyde in the sample). Aliquots of 25 mL were settled for 24 h in an Utermöhl chamber (Hydro-Bios GmbH, Germany) and species were identified and enumerated using an inverted microscope (Leica, model DM IL, Germany) following the technique described by Villafañe and Reid (1995). The biovolumes of the phytoplankton species were estimated by adjusting their shape to known geometric forms following Hillebrand et al. (1999), and by measuring the main cell dimensions of at least 10 cells per species. From these biovolumes, C biomass was calculated with the equations of Strathmann (1967).

For APP and HPP, 1.5 mL of sample was fixed with 75 μL of particle-free 20% (w/v) paraformaldehyde (1% final concentration) and stored at 4°C until analysis to quantify cell abundance using a flow cytometer (FACSCanto II, Becton Dickinson Biosciences, Oxford, UK). Prior to analysis, all samples were stained with Syber Green I DNA (Sigma-Aldrich Co Ltd) 1 : 5000 final dilution (Gasol and Del Giorgio 2000; Zubkov et al. 2007). After this, yellow-green 1-μm beads at standard concentration (Fluoresbrite Microparticles, Polysciences, Pennsylvania, U.S.A.) were also added to determine the absolute cellular concentration (Zubkov and Burkill 2006; Zubkov et al. 2007). As with the same samples we quantified APP and HPP, we used the phycoerythrin and Chl *a* signals to distinguish between autotrophic and heterotrophic picoplankton groups (Mercado et al. 2006). From cell abundance values we estimated the biovolumes of both picoplanktonic groups following Zubkov et al. (1998), which were converted into C biomass by using conversion factors of 0.22 (Booth 1988) and 0.35 pg C μm^{-3} (Bjørnsen 1986) for the APP and HPP fractions, respectively.

Growth rates

The specific growth rates of ANP, APP, and HPP (μ, in d^{-1}) under the different experimental conditions were calculated from cell concentration as:

$$\mu = \ln\ (N_5/N_1)/(t_5 - t_1) \quad (1)$$

where N_5 is the cellular concentration (in cells $mL^{-1} \times 10^3$) the last day of the experiment (t_5) and N_1 is the cell concentration at the first day of the experiment (t_1).

O_2 concentration measurements

Samples from each microcosm were taken daily (before sunrise) and placed into Teflon FEP narrow-mouth bottles (Nalgene®-35 mL) without bubbles. Each Teflon bottle (18 in total), equipped with an O_2 sensor-spot (SP-PSt3-NAU-D5-YOP, PreSens GmbH, Germany), was exposed to the same radiation treatment as that imposed on the corresponding mesocosm from which it came and were placed inside a water bath to maintain the in situ temperature. The O_2 concentrations were measured during 24 daily cycles using a Fibox 3 optode-probe oxygen transmitter (PreSens GmbH, Germany) furnished with the Oxyview 6.02 software and a fibre-optic. Measurements started at dawn and were made hourly until dusk (seven measurements), and then every 4–6 h during the night (4–5 measurements) until completing the daily cycle. Each sample was measured for 30 s, collecting one datum per second. Every day, before the measurements, the probe was calibrated using a two-point (0% and 100% saturation) calibration procedure, at the in situ temperature and taking into account the atmospheric pressure.

Fluorescence measurements

To determine the dynamics of Φ_{PSII} over the experimental period, aliquots of 3-mL were taken daily from each microcosm at dawn, noon and dusk (18 samples and three times per day = 54 samples in total/day) to measure the in vivo PSII photochemical parameters using a pulse amplitude modulated (PAM) fluorometer (Walz, Water PAM, Effeltrich, Germany). Each sample was measured six times immediately after sampling, without any dark-adaptation, with each measurement lasting 10 s; thus the total time for measuring each sample was 1 min. The effective photochemical quantum yield of PSII was calculated using the equations of Genty et al. (1989) and Maxwell and Johnson (2000) as:

$$\Phi_{PSII} = \Delta F/F'_m = \left(F'_m - F_t\right)/F'_m \quad (2)$$

where F'_m is the maximum fluorescence induced by a saturating light pulse (ca. 5300 μmol photons $m^{-2}\ s^{-1}$ in 0.8 s) and F_t the current steady-state fluorescence induced by a red actinic light pulse (492.2 μmol photons $m^{-2}\ s^{-1}$ – peak at 660 nm) in light-adapted cells.

Data and statistical analyses

From monthly POC data, we fitted a linear regression model POC vs. time for the 1997–2014 and 2015–2016 period to evaluate long-term trends over the time before and after the experimental study in SAO. In addition, from daily light-darkness Φ_{PSII} measurements, we fitted a polynomial regression model to the values at noon and dawn vs. time for each radiation and nutrient treatment to assess: (1) the Φ_{PSII} inhibition undergone by the communities at noon when received maximal irradiances; and (2) the dark recovery capacity of these communities from the dusk to the following dawn to counteract the potential photodamage experienced during the previous day.

Likewise, we also fitted a polynomial regression model with oxygen concentration values at noon vs. time for each radiation and nutrient treatment to calculate the changes in the net primary production (NPP, in mmol $O_2\ m^{-3}\ d^{-1}$) throughout the experiment as:

$$NPP = [O_2]_{t5} - [O_2]_{t1}/t_5 - t_1 \quad (3)$$

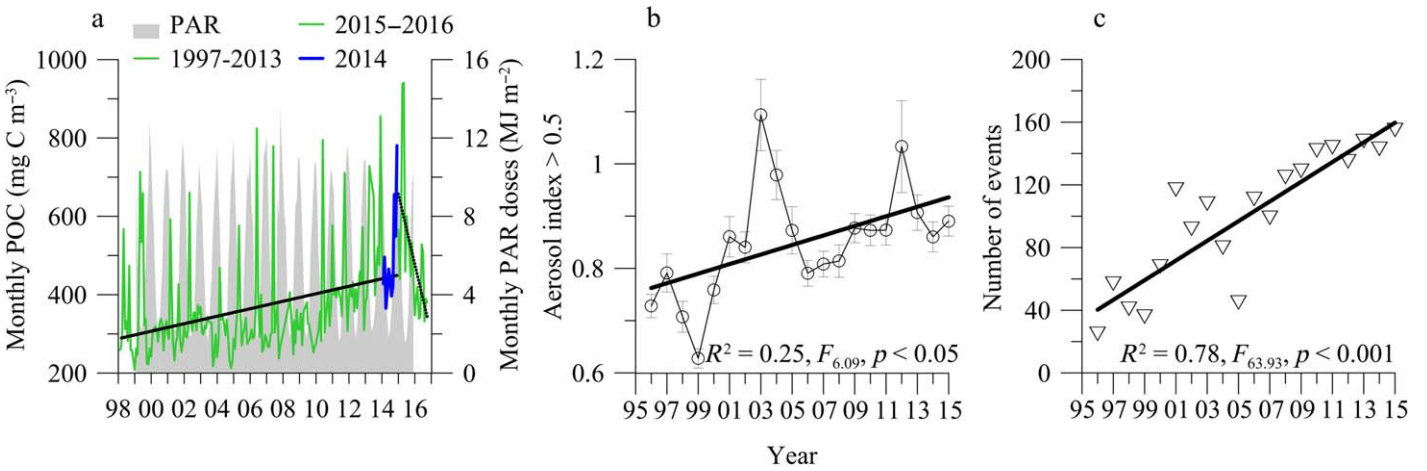

Fig. 1. (**a**) Mean (± SD) monthly particulate organic carbon (POC, in mg C m^{-3}; green line) for from 1997 to 2016 and monthly photosynthetically active radiation doses (PAR, in MJ m^{-2}; gray areas) from 1999 to 2015 period. Solid blue line represent the experimental year (2014). (**b**) Mean (± SD) annual aerosol index > 0.5 (AI, relative units) and (**c**) total number of AI > 0.5 events from 1995 to 2015 period on Egi station (43° 18.8′S, 65° 02.0′W). Solid (1997–2014) and dashed (2015–2016) lines represent the linear regression fits. [Color figure can be viewed at wileyonlinelibrary.com]

$[O_2]_{t5}$ being the O_2 concentrations modeled on the last day of the experiment (t_5) and $[O_2]_{t1}$ the concentrations for modeled the first day (t_1) of exposure.

From the O_2 concentrations measured during the night, we calculated the dark community respiration (CR_{dark}, in mmol m^{-3} d^{-1}) for each radiation and nutrient treatment throughout the experiment as the difference between the O_2 concentrations measured before dawn of the following experimental day and those measured during the dusk of the experimental day considered. From daily data, we integrated over the week at the same way than for NPP.

Then, we assessed the effect size of UVR on NPP and CR_{dark} under ambient, dust or riverine treatments as:

$$\text{Effect size of UVR } (\%) = (X_P - X_{PAB})/X_P \times 100 \quad (4)$$

with X being the NPP or CR_{dark} under UVR + PAR (PAB) and only PAR (P) treatments, respectively. Note that positive values denote an inhibitory effect, whereas negative values a stimulation of the considered process.

The daily CR rates (mmol O_2 m^{-3}d^{-1}) for each nutrients treatment and day were calculated as:

$$\text{Daily CR} = \text{CR}_{\text{darkPAB}} + \text{light CR} \quad (5)$$

where the $CR_{darkPAB}$, represents the respiration values measured during the night in samples previously exposed to full solar radiation. The light CR was estimated after obtaining the effect size of UVR (Eq. 4) on respiration and applying this factor to the $CR_{darkPAB}$ as:

$$\text{Light CR} = \text{CR}_{\text{darkPAB}} \times (1 - \text{Effect size of UVR}) \quad (6)$$

By doing so, we had more realistic measurements of daily CR, as other experimental studies (Agustí et al. 2014; Medina-Sánchez et al. 2017) have shown that the respiration rates of planktonic communities can be enhanced or inhibited under UVR exposure. Finally, we estimated the gross primary production (GPP) under ambient, dust, and riverine treatments as:

$$\text{GPP} = \text{NPP} + (\text{daily}_{\text{CRPAB}}) \quad (7)$$

From the GPP and daily CR_{PAB} (*see* Supporting Information Table S2) data we evaluated the CO_2-sink capacity of our model coastal ecosystem, as the ratio between the two parameters, under ambient, dust, and riverine treatments after an acclimation period of 5 d.

We used a two-way analysis of the variance (ANOVA) to test the interactions between UVR and nutrient (amb, dust, and riv) treatments on NPP, CR_{dark}, cell abundances, and growth rates of ANP, APP, and HPP. We also used a one-way ANOVA to test significant differences between nutrient treatments on the effect size of UVR (%) on NPP and CR_{dark}, on daily CR and on CO_2-sink capacity. Normality (by Shapiro-Wilk's test) and homoscedasticity (by Levene's test) or sphericity (by Mauchly's test) was checked for each variable to verify the ANOVA and RM-ANOVA assumptions (Zar 1999). When interactive effects were significant, least significant differences (LSD) Fisher post hoc tests were performed. Student's tests were used to test significant differences between the slopes of the polynomial regression fits of Φ_{PSII}. All data are reported as mean and standard deviation, whereas error propagation was used to calculate the error for the effect size of UVR (%) on NPP and CR_{dark}.

Results

Long-term trends in POC and AI on coastal South Atlantic Ocean waters

The monthly POC exhibited a characteristic response pattern throughout the 1997–2016 period (Fig. 1a), with increasing

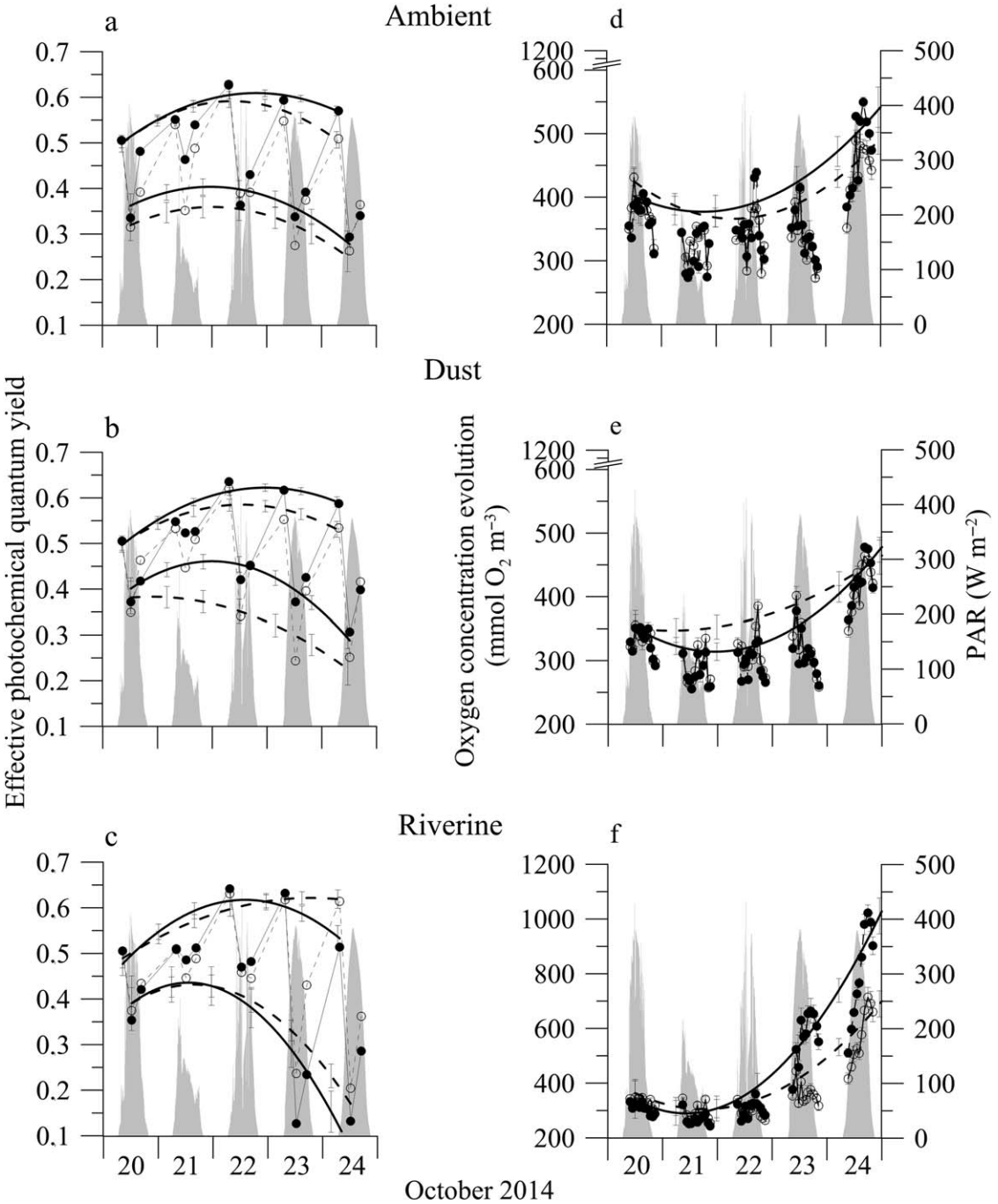

Fig. 2. Daily cycles of mean values (± SD) of effective photochemical quantum yield (**a**–**c**) and oxygen concentration evolution (**d**–**f**) in planktonic communities exposed to two radiation treatments, PAB (> 280 nm, open circles) and P (PAR, > 400 nm, solid circles) and three nutrient treatments, ambient, dust, and riverine inputs during the experimental period (20–24th October). Gray areas represent daily irradiances of photosynthetically active radiation (PAR, in W m^{-2}). Dashed (samples under PAB) and solid (samples under P) lines represent the polynomial regression fit at during the incubation period whereas the vertical lines represent the 95% confidence intervals. Note that for panels (**a**–**c**) the polynomial regression fits were done at dawn and at noon.

concentrations coupled with decreasing monthly PAR doses within each year (maximal peaks ranging between ~ 600 mg C m^{-3} and 1000 mg C m^{-3}) followed by decreasing POC values that matched increasing monthly PAR doses. Despite these variable inter-annual trends, our results showed a steady increase in POC over the time which lasted up to 2014 ($R = 0.41$, $F_{5.11}$, $p < 0.001$). Noticeably, this trend was significantly inverted ($R = -0.59$, $F_{0.01}$, $p < 0.001$) in the last 2 yr

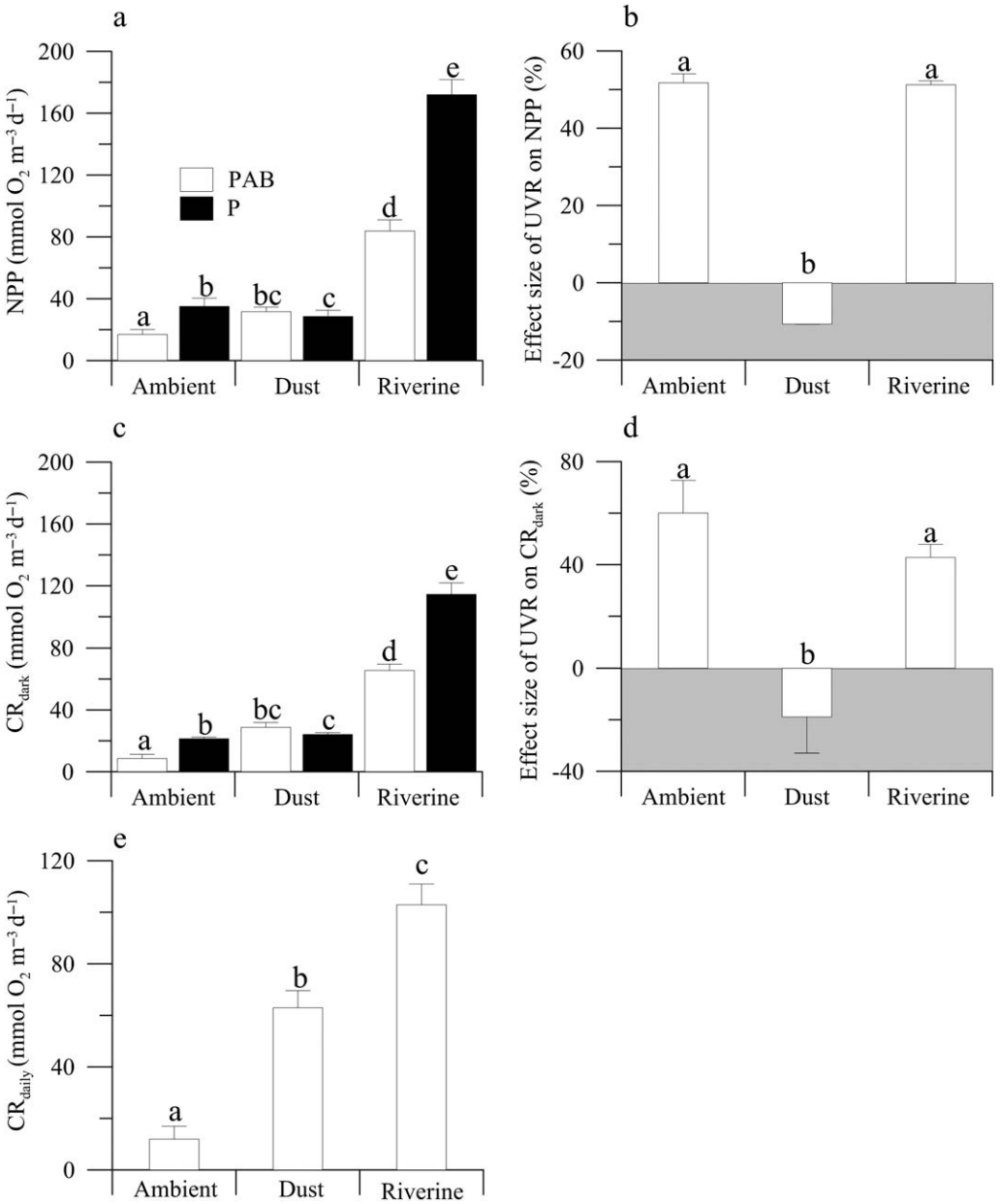

Fig. 3. (**a**) Mean (± SD) net primary production (NPP, in mmol O_2 m^{-3} d^{-1}) and (**c**) dark community respiration (CR_{dark}, in mmol O_2 m^{-3} d^{-1}) rates in samples exposed to two radiation treatments, PAB (> 280 nm) and P (PAR, > 400 nm), and three nutrient treatments, ambient, dust, and riverine over the experimental period (20–24th October). Mean (± SD) effect size of UVR (%) on the total NPP (**b**) and CR_{dark} (**d**) under ambient, dust, and riverine treatments. (**e**) Daily CR rates (in mmol O_2 m^{-3} d^{-1}) under ambient dust and riverine treatments over the experimental period. The letters on the top of bars indicate significant differences by the least significant differences post hoc test.

(2015–2016). Likewise, the AI values showed both the intensity and the frequency of these events significantly increased from 1997 until present on this coastal area (AI > 0.5, Fig. 1b,c).

Photosynthetic activity and planktonic metabolic responses

Our experimental manipulation determined a typical V-shaped pattern of Φ_{PSII} over daily light-dark periods, with decreases in Φ_{PSII} as light intensities increased during the day followed by increases in Φ_{PSII} at lower light intensities during the evening (Fig. 2a–c; Supporting Information Table S1). Thus, the highest photoinhibition of PSII occurred at noon when the communities received maximal radiation levels. In addition, this inhibition was particularly high during the last 2 d, when the maximal mean irradiance values were registered. In fact, whereas the mean daily irradiance values were ca. 152.21 W m^{-2} and 0.50 W m^{-2} during the three first days, they reached ca. 223 W m^{-2}, 32 W m^{-2}, and 0.70 W m^{-2} during the last 2 d of the experiment, for PAR, UV-A,

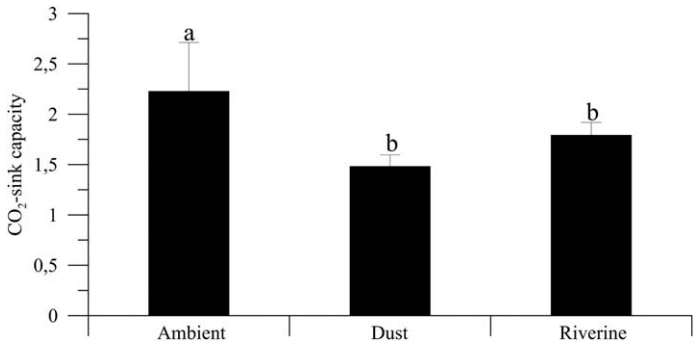

Fig. 4. Mean (± SD) CO_2-sink capacity in coastal waters of the South Atlantic Ocean after an acclimation period of 5 d under ambient, dust, and riverine inputs. The letters on the top of bars indicate significant differences by least significant differences post hoc test.

and UV-B, respectively. Moreover, this greater photoinhibition found toward the end of the experiment was dependent not only on the radiation treatment but also on the nutrient source considered. In this sense, we found that the noon Φ_{PSII} values decreased twofold (from ~ 0.36 to 0.17) under riverine treatments regardless of the radiation treatment considered (Fig. 2c; Supporting Information Table S1). Also, we found that the noon Φ_{PSII} values were significantly lower (twofold) under these conditions than under dust or ambient treatments (Fig. 2a,b) where they had values ~ 0.33, on average, during the same period (*t*-test riv vs. amb = 6.92, $p < 0.001$; *t*-test riv vs. dust = 3.62, $p < 0.001$). Conversely, dawn Φ_{PSII} exhibited similar or even higher values (between ~ 0.5 and 0.6) over the experiment, particularly under riverine treatments (with one exception, day 24 in P_{riv}), denoting that night recovery was enough to counteract the daily inhibition, avoiding any chronic damage to the PSII.

The O_2 time course also exhibited a response modulated by the daily light-dark cycles. During the first 3 d, these O_2 cycles showed a fluctuating response due to the dominating cloudy conditions; by contrast, during the last 2 d these cycles exhibited a characteristic response pattern with increases from dawn to dusk, followed by a continuous decrease during the darkness period (Fig. 2d–f; Supporting Information Table S1). The O_2 concentrations showed an increasing trend over the experiment, which were steeper under riverine (> 500 mmol O_2 m^{-3}; Fig. 2f) than under ambient or dust treatments (~ or < 500 mmol O_2 m^{-3}). Regarding to the NPP, our results showed a significant UVR × Nut interactive effect ($F_{2424.59}$, $p < 0.001$); thus, the NPP was 2- to 4-fold higher under riverine treatments than in ambient and dust conditions (~ 40 mmol O_2 $m^{-3}d^{-1}$; Fig. 3a). However, the UVR exerted a similar inhibitory effect (~ 50%) on NPP under ambient and riverine treatments, but it significantly augmented (ca. −10%) under dust treatments (Fig. 3b).

In the same way as for NPP, there was a significant UVR × Nut interaction over the experiment on CR_{dark} ($F_{74.92}$, $p < 0.001$). In fact, we also found that CR_{dark} was 3- to 6-fold higher under riverine than in ambient and dust treatments (Fig. 3c). In addition, when we evaluated how the previous UVR exposure could alter the CR_{dark} in our nutrient-enriched treatments, our results evidenced that dust addition significantly stimulated (ca. −20%), whereas that riverine inputs inhibited, reaching similar inhibition values as those found under ambient conditions (~ 50% on average; Fig. 3d). However, when we studied how these nutrient treatments affected the daily CR rates over the experiment, we found that whereas the former significantly increased the latter (LSD post hoc, $p < 0.001$), these rates were significantly fourfold higher under riverine than under dust treatments Fig. 3e).

Plankton metabolic balance: nutrients source and UVR interaction

The CO_2-sink capacity showed values > 1 in all treatments, indicating a net autotrophic metabolism in our coastal model ecosystem (Fig. 4; Supporting Information Table S2). Nevertheless, we found significant decreases in the CO_2-sink capacity for the dust and riverine treatments as compared to ambient conditions. In fact, at the end of the experimental period these decreases in the sink capacity indicate a significant reduction of the CO_2 uptake by communities acclimated to the future conditions, by as much as ~ 27% on average, regardless of the nutrient source considered.

Plankton community structure

After 5 d of acclimation, there were significant shifts in the planktonic community structure as opposed to the interaction UVR × dust or riverine; thus, whereas the HPP abundances markedly declined over the experiment and the APP fraction did not vary during this period, ANP abundance significantly augmented (Supporting Information Figs. S1a, S2). Moreover, ANP and HPP showed significantly higher abundance values in samples receiving only PAR, regardless the nutrient treatment, whereas APP abundance showed the opposite pattern (except under ambient nutrients; Supporting Information Fig. S1a). These shifts in the autotrophic fraction over the experiment were coupled with increasing Chl *a* concentrations, which were on average fourfold higher (~ 88 mg m^{-3} vs. ~ 20 mg m^{-3}; Supporting Information Table S3) under riverine than under ambient and dust treatments.

These diverse responses of the cell abundance resulted in different nano- and picoplanktonic growth rates (Supporting Information Fig. S1b), exhibiting positive values in the ANP (~ 1.5 d^{-1}) and negative in the HPP (–0.5 d^{-1}). Notwithstanding, whereas the dust and riverine inputs counteracted the negative UVR effects on ANP growth, both nutrients accentuated them in HPP growth (Supporting Information Fig. S1b). APP did not show a clear response either to radiation or to nutrient treatments. In terms of biomass, the plankton community was co-dominated by autotrophs and heterotrophs at the beginning of the experiment; however, after 5 d of acclimation, ANP greatly increased (~ 85–95%) compared to the APP and HPP fractions regardless the

treatment considered (Supporting Information Fig. S1c). Within the ANP fraction, unidentified flagellates < 10 μm dominated or co-dominated the community as opposed to diatoms (mainly pennates). The contribution of dinoflagellates was almost negligible ($< 1\%$ of the total biomass) in all treatments. These shifts in the plankton community resulted in acute drops in the nutrient concentrations throughout the experiment. In fact, under ambient and dust input treatments, such concentrations ranged from $\sim$ 2.60 μM and 2.34 μM at the beginning of the experiment to 0.03 μM and 0.40 μM at the end for N and P, respectively. For Si, we found a moderate consumption between $\sim$ 25 (amb and dust) and 50% (riv) with respect to the initial conditions (data not shown).

Discussion

This study reports for the first time a potential reduction of the CO_2-sink capacity of coastal waters of SAO by an increase in nutrients either through aeolian-dust deposition or riverine discharge under high UVR fluxes. Despite the consistent impact of both drivers acting together on the planktonic metabolic balance, we found that UVR exerted a stimulatory effect on NPP and CR under dust inputs but inhibitory under riverine treatments. The underlying mechanism that can explain this stimulatory effect on both metabolic processes after aeolian-dust inputs is the lower dynamic photoinhibition of phytoplankton communities found under these conditions together with an enhanced dark recovery. This latter mechanism, dark recovery, would divert part of the energy expenditure (e.g., through respiration) of planktonic organisms toward protein and ATP synthesis rather than PSII repair, and thus, it would permit an increase the photosynthetic activity (Li et al. 2016).

These findings partially contrast with recent reports showing a consistent inhibitory UVR effect on PP and CR after aeolian-dust inputs (Cabrerizo et al. 2016), and on PP after nutrient inputs (Carrillo et al. 2008, 2015). A plausible explanation to these contrasting results may lie in the different trophic state of the two marine areas considered, a highly productive and non-limited by nutrients in the case of the coastal SAO vs. an unproductive and strongly nutrient-limited (mainly P) area in the case of the south-western coast of the Mediterranean Sea.

Surprisingly, although the joint action of UVR $\times$ dust or riverine was opposite on the metabolism of planktonic communities (see above), we found that it was translated into a similar shift in the structure of the planktonic community toward a dominance by nanoplanktonic flagellates. The specific reasons why nanoflagellates dominated the community regardless of the nutrient source considered might include the following: (1) higher metabolic demands and nutrient uptake when nutrient availability increases (Roberts and Howarth 2006; Mercado et al. 2014); (2) their active movement capacity, which could confer them a competitive advantage under shallow and stable UML conditions, as found in our study, compared with organisms lacking this capacity (e.g., diatoms) (Striebel et al. 2009); and (3) their potential ability to combine two metabolisms, one phototrophic to obtain carbon and other phagotrophic to obtain limiting nutrients, into the same organism to grow (Raven 1997; Fischer et al. 2017). Despite that we did not quantify mixotrophy *sensu stricto*, we found a consistent decrease of the HPP compartment throughout the incubation period. This decline observed in HPP suggests potential bacterivory by flagellates. Nevertheless, we can rule out that toxic elements and heavy metals (e.g., Pb, Cu) carried by the dust may have interfered with the planktonic metabolism and growth (e.g., HPP) (Paytan et al. 2009; Jordi et al. 2012) and, consequently, may have influenced the CO_2-sink capacity of the ecosystem with respect to the riverine treatments. In fact, we found that the concentration of such elements were below the detection limits, in agreement with recent reports showing no significant amount of these elements after dust deposition (González-Olalla et al. 2017).

The decreased sink capacity found in SAO under enriched nutrient conditions and high UVR levels is lower than those that predict reductions in the C-downward fluxes between 38% and 50% in surface waters of ecosystems in low (LNLC) and high (HNLC) latitudes, respectively (Boyd 2015). Moreover, the Boyd model simulations, which included more 10 biotic and abiotic factors, revealed that changes in the phytoplankton community structure had the greatest single effect on C fluxes in the future ocean (Boyd 2015). Thus, the consistent response pattern reported in our study between flagellate-dominated communities and decreased CO_2-sink capacity under both global-change scenarios assayed could support the Boyd's proposal. In addition, the estimates provided here regarding the planktonic metabolic balance agree with the values reported in previous observational studies both in temperate and in tropical ecosystems of both Hemispheres (GPP/CR $= \sim 1.5$), although they are between 3- and 5-fold lower than those found in polar ecosystems, possibly due to the fact that these studies were performed mostly during continuous spring-summer daylight (Regaudie-de-Gioux and Duarte 2013).

Considering all the above-mentioned findings, we can postulate that the nutrient enrichment of coastal ecosystems, which comprise only 5% of the total oceanic area, could drive that a high C-fixed fraction by phytoplankton photosynthesis to be respired and released as CO_2 into the atmosphere in the future, thus weakening the current role that these key buffers possess in the global C cycle as strong CO_2 sinks (Padín et al. 2010; Bauer et al. 2013). Notwithstanding, recent results by Bermejo et al. (2018) also show that other abiotic factors such as present-day shifts in the wind patterns can influence the trends observed, delaying and weakening the timing as well as the intensity, respectively, of the phytoplankton bloom in the SAO. This likely decline in C uptake proposed in this study for coastal waters

of SAO could sustain the recent decreases that are being registered in the area in terms of POC (Fig. 1a) which subsequently are also triggering significant decreases in fishing catches (Economía and Regiones 2016).

Conclusions

Although we are fully aware that our experimental setup simulates extreme events of nutrients inputs under high UVR irradiance and it was performed at a specific time, they offer realism and ecological significance because: (1) the longer-term scales (> 1 d) avoided bias in the estimates of the metabolic balance of ecosystems which traditionally has been evaluated through short-term scales (< day, *see* Duarte et al. 2013; Regaudie-de-Gioux and Duarte 2013) and (2) the study combines both the plankton metabolic status (García-Corral et al. 2017) as well as the shifts in the plankton community structure (Villafañe et al. 2017),which are usually neglected in these types of metabolic studies. Therefore, as we are now at an unprecedented juncture in the field of the global-change ecology, the integration of both mid-term experimental approaches together with long-term remote-sensing and observational data implies an improvement in the understanding about how the increasing climatic variability that the marine ecosystems are undergoing could have severe impact on their capacity to sequester CO_2 in the future.

References

Acha, E. M., H. Mianzan, R. A. Guerrero, M. Favero, and J. Bava. 2004. Marine fronts at the continental shelves of austral South America: Physical and ecological processes. J. Mar. Syst. **44**: 83–105. doi:10.1016/j.jmarsys.2003.09.005

Acker, J. G., and G. Leptoukh. 2007. Online analysis enhance NASA Earth science data. EOS Trans. Am. Geophys. Union **88**: 14–17. doi:10.1029/2007EO020003

Agustí, S., A. Regaudie-de-Gioux, J. M. Arrieta, and C. M. Duarte. 2014. Consequences of UV-enhanced community respiration for plankton metabolic balance. Limnol. Oceanogr. **59**: 223–232. doi:10.4319/lo.2014.59.1.0223

Bauer, J. E., W.-J. Cai, P. A. Raymond, T. S. Bianchi, C. S. Hopkinson, and P. A. G. Regnier. 2013. The changing carbon cycle of the coastal ocean. Nature **504**: 61–70. doi:10.1038/nature12857

Bermejo, P., E. W. Helbling, C. Durán-Romero, M. J. Cabrerizo, and V. E. Villafañe. 2018. Abiotic control of phytoplankton blooms in temperate coastal marine ecosystems: A case study in the South Atlantic Ocean. Sci. Total Environ. **612**: 894–902. doi:10.1016/j.scitotenv.2017.08.176

Bianchi, A. A., and others. 2009. Annual balance and seasonal variability of sea-air CO_2 fluxes in the Patagonia Sea: Their relationship with fronts and chlorophyll distribution. J. Geophys. Res. **114**: C03018. doi:10.1029/2008JC004854

Björn, L. O., and T. M. Murphy. 1985. Computer calculation of solar ultraviolet radiation at ground level. Physiol. Veg. **23**: 555–561.

Bjørnsen, P. K. 1986. Automatic determination of bacterioplankton biomass by image analysis. Appl. Environ. Microbiol. **51**: 1199–1204.

Booth, B. C. 1988. Size classes and major taxonomic groups of phytoplankton at two locations in the subarctic Pacific Ocean in May and August, 1984. Mar. Biol. **97**: 275–286. doi:10.1007/BF00391313

Boyd, P. W. 2015. Toward quantifying the response of the oceans' biological pump to climate change. Front. Mar. Sci. **2**: 77. doi:10.3389/fmars.2015.00077

Brahney, J., N. Mahowald, D. S. Ward, A. P. Ballantyne, and J. C. Neff. 2015. Is atmospheric phosphorus pollution altering global alpine Lake stoichiometry? Global Biogeochem. Cycles **29**: GB5137. doi:10.1002/2015GB005137

Browning, T. J., H. A. Bouman, G. M. Henderson, T. A. Mather, D. M. Pyle, C. Schlosser, E. M. S. Woodward, and C. M. Moore. 2014. Strong responses of Southern Ocean phytoplankton communities to volcanic ash. Geophys. Res. Lett. **41**: 2851–2857. doi:10.1002/2014GL059364

Bullard, J. E., and others. 2016. High-latitude dust in the Earth system. Rev. Geophys. **54**: 47–485. doi:10.1002/2016RG000518

Bullejos, F. J., P. Carrillo, M. Villar-Argaiz, and J. M. Medina-Sánchez. 2010. Roles of phosphorus and ultraviolet radiation in the strength of phytoplankton–zooplankton coupling in a Mediterranean high mountain lake. Limnol. Oceanogr. **55**: 2549–2562. doi:10.4319/lo.2010.55.6.2549

Cabrerizo, M. J., J. M. Medina-Sánchez, J. M. González-Olalla, M. Villar-Argaiz, and P. Carrillo. 2016. Saharan dust and high UVR jointly alter the metabolic balance in marine oligotrophic ecosystems. Sci. Rep. **6**: 35892. doi:10.1038/srep35892

Carrillo, P., J. A. Delgado-Molina, J. M. Medina-Sánchez, F. J. Bullejos, and M. Villar-Argaiz. 2008. Phosphorus inputs unmask negative effects of ultraviolet radiation on algae in a high mountain lake. Glob. Chang. Biol. **14**: 423–439. doi:10.1111/j.1365-2486.2007.01496.x

Carrillo, P., and others. 2015. Interactive effect of UVR and phosphorus on the coastal phytoplankton community of the Western Mediterranean Sea: Unravelling ecophysiological mechanisms. Plos One **10**: e0142987. doi:10.1371/journal.pone.0142987

Dao, L. H. T., and J. Beardall. 2016. Effects of lead on growth, photosynthetic characteristics and production of reactive oxygen species of two freshwater green algae. Chemosphere **147**: 420–429. doi:10.1016/j.chemosphere.2015.12.117

Duarte, C. M., A. Regaudie-de-Gioux, J. M. Arrieta, A. Delgado-Huertas, and S. Agustí. 2013. The oligotrophic ocean is heterotrophic. Ann. Rev. Mar. Sci. **5**: 551–569. doi:10.1146/annurev-marine-121211-172337

Economía and Regiones. 2016. Informe de actividad marítima pesquera, p. 1–6.

Fischer, R., H.-A. Giebel, H. Hillebrand, and R. Ptacnik. 2017. Importance of mixotrophic bacterivory can be predicted by light and loss rates. Oikos **126**: 713–722. doi:10.1111/oik.03539

García-Corral, L. S., and others. 2017. Effects of UVB radiation on net community production in the upper global ocean. Glob. Ecol. Biogeogr. **26**: 54–64. doi:10.1111/geb.12513

Gasol, J. M., and P. Del Giorgio. 2000. Using flow cytometry for counting natural planktonic bacteria and understanding the structure of planktonic bacterial communities. Sci. Mar. **64**: 197–224. doi:10.3989/scimar.2000.64n2197

Genty, B. E., J. M. Briantais, and N. R. Baker. 1989. The relationship between the quantum yield of photosynthetic electron transport and quenching of chlorophyll fluorescence. Biochim. Biophys. Acta **990**: 87–92. doi:10.1016/S0304-4165(89)80016-9

González-Olalla, J. M., J. M. Medina-Sánchez, M. J. Cabrerizo, M. Villar-Argaiz, P. M. Sánchez-Castillo, and P. Carrillo. 2017. Contrasting effect of Saharan dust and UVR on autotrophic picoplankton in nearshore vs. offshore waters of Mediterranean Sea. J. Geophys. Res. Biogeosci. **122**: 2085–2103. doi:10.1002/2017JG003834

Guerzoni, S., E. Molinaroli, and R. Chester. 1997. Saharan dust inputs to the western Mediterranean Sea: Depositional patterns, geochemistry and sedimentological implications. Deep-Sea Res. Part II **44**: 631–654. doi:10.1016/S0967-0645(96)00096-3

Guieu, C., and others. 2010. Large clean mesocosms and simulated dust deposition: A new methodology to investigate responses of marine oligotrophic ecosystems to atmospheric inputs. Biogeosciences **7**: 2765–2784. doi:10.5194/bg-7-2765-2010

Harding, L. W., C. L. Gallegos, E. S. Perry, W. D. Miller, J. E. Adolf, M. E. Mallonee, and H. W. Paerl. 2016. Long-term trends of nutrients and phytoplankton in Chesapeake Bay. Estuaries Coast. **39**: 664–681. doi:10.1007/s12237-015-0023-7

Harrison, J. W., G. M. Silsbe, and R. E. H. Smith. 2015. Photophysiology and its response to visible and ultraviolet radiation in freshwater phytoplankton from contrasting light regimes. J. Plankton Res. **37**: 472–488. doi:10.1093/plankt/fbv003

Helbling, E. W., E. S. Barbieri, M. A. Marcoval, R. J. Gonçalves, and V. E. Villafañe. 2005. Impact of solar ultraviolet radiation on marine phytoplankton of Patagonia, Argentina. Photochem. Photobiol. **81**: 807–818. doi:10.1562/2005-03-02-RA-452

Helbling, E. W., D. E. Pérez, C. D. Medina, M. G. Lagunas, and V. E. Villafañe. 2010. Phytoplankton distribution and photosynthesis dynamics in the Chubut River estuary (Patagonia, Argentina) throughout tidal cycles. Limnol. Oceanogr. **55**: 55–65. doi:10.4319/lo.2010.55.1.0055

Helbling, E. W., A. T. Banaszak, and V. E. Villafañe. 2015. Global change feed-back inhibits cyanobacterial photosynthesis. Sci. Rep. **5**: 14514. doi:10.1038/srep14514

Hessen, D. O., H. Frigstad, P. J. Færøvig, M. W. Wojewodzic, and E. Leu. 2012. UV radiation and its effects on P-uptake in arctic diatoms. J. Exp. Mar. Biol. Ecol. **411**: 45–51. doi:10.1016/j.jembe.2011.10.028

Hillebrand, H., C. D. Dürselen, D. Kirschtel, U. Pollingher, and T. Zohary. 1999. Biovolume calculation for pelagic and benthic microalgae. J. Phycol. **35**: 403–424. doi:10.1046/j.1529-8817.1999.3520403.x

Hoffmann, L. J., E. Breitbarth, M. V. Ardelan, S. Duggen, N. Olgun, M. Hassellöv, and S.-Å. Wängberg. 2012. Influence of trace metal release from volcanic ash on growth of *Thalassiosira pseudonana* and *Emiliania huxleyi*. Mar. Chem. **132–133**: 28–33. doi:10.1016/j.marchem.2012.02.003

Holm-Hansen, O., and B. Riemann. 1978. Chlorophyll *a* determination: Improvements in methodology. Oikos **30**: 438–447. doi:10.2307/3543338

Jeffrey, W. H., J. P. Kase, and S. W. Wilhelm. 2000. Ultraviolet radiation effects on bacteria and viruses in marine ecosystems, p. 206–236. *In* S. de Mora, S. Demers, and M. Vernet [eds.], The effects of UV radiation on marine ecosystems. Cambridge Univ. Press.

Jickells, T. D., and C. M. Moore. 2015. The importance of atmospheric deposition for ocean productivity. Annu. Rev. Ecol. Evol. Syst. **46**: 481–501. doi:10.1146/annurev-ecolsys-112414-054118

Jordi, A., G. Basterretxea, A. Tovar-Sánchez, A. Alastuey, and X. Querol. 2012. Copper aerosols inhibit phytoplankton growth in the Mediterranean Sea. Proc. Natl. Acad. Sci. USA **109**: 21246–21249. doi:10.1073/pnas.1207567110

Lekunberri, I., and others. 2010. Effects of a dust deposition event on coastal marine microbial abundance and activity, bacterial community structure and ecosystem function. J. Plankton Res. **32**: 381–396. doi:10.1093/plankt/fbp137

Li, G., A. D. Woroch, N. A. Donaher, A. M. Cockshutt, and D. A. Campbell. 2016. A hard day's night: Diatoms continues recycling Photosystem II in the dark. Front. Mar. Sci. **3**: 218. doi:10.3389/fmars.2016.00218

Maar, M., S. Markager, K. S. Madsen, J. Windolf, M. M. Lyngsgaard, H. E. Andersen, and E. F. Møller. 2016. The importance of local versus external nutrient loads for Chl *a* and primary production in the Western Baltic Sea. Ecol. Modell. **320**: 258–272. doi:10.1016/j.ecolmodel.2015.09.023

Macías, D., E. Ramírez-Romero, and C. M. García. 2010. Effect of nutrient input frequency on the structure and dynamics of the marine pelagic community: A modeling approach. J. Mar. Res. **68**: 119–151. doi:10.1357/002224010793078979

Mahowald, N., and others. 2008. Global distribution of atmospheric phosphorus sources, concentrations and

deposition rates, and anthropogenic impacts. Global Biogeochem. Cycles **22**: GB4026. doi:10.1029/2008GB003240

Marañón, E., and others. 2010. Degree of oligotrophy controls the response of microbial plankton to Saharan dust. Limnol. Oceanogr. **55**: 2339–2352. doi:10.4319/lo.2010.55.6.2339

Marcoval, M. A., V. E. Villafañe, and E. W. Helbling. 2008. Combined effects of solar ultraviolet radiation and nutrients addition on growth, biomass and taxonomic composition of coastal marine phytoplankton communities of Patagonia. J. Photochem. Photobiol. B Biol. **91**: 157–166. doi:10.1016/j.jphotobiol.2008.03.002

Martínez-García, S., E. Fernández, A. Calvo-Díaz, P. Cermeño, E. Marañón, X. A. G. Morán, and E. Teira. 2013. Differential response of microbial plankton to nutrient inputs in oligotrophic versus mesotrophic waters of the North Atlantic. Mar. Biol. Res. **9**: 358–370. doi:10.1080/17451000.2012.745002

Maxwell, K., and G. N. Johnson. 2000. Chlorophyll fluorescence - a practical guide. J. Exp. Bot. **51**: 659–668. doi:10.1093/jexbot/51.345.659

Medina-Sánchez, J. M., G. Herrera, C. Durán, M. Villar-Argaiz, and P. Carrillo. 2017. Optode use to evaluate microbial planktonic respiration in oligotrophic ecosystems as an indicator of environmental stress. Aquat. Sci. **79**: 529–541. doi:10.1007/s00027-016-0515-y

Mercado, J. M., T. Ramírez, D. Cortés, M. Sebastián, A. Reul, and B. Bautista. 2006. Diurnal changes in the bio-optical properties of the phytoplankton in the Alborán Sea (Mediterranean Sea). Estuar. Coast. Shelf Sci. **69**: 459–470. doi:10.1016/j.ecss.2006.05.019

Mercado, J. M., I. Sala, S. Salles, D. Cortés, T. Ramírez, E. Liger, L. Yebra, and B. Bautista. 2014. Effects of community composition and size structure on light absorption and nutrient uptake of phytoplankton in contrasting areas of the Alboran Sea. Mar. Ecol. Prog. Ser. **499**: 47–64. doi:10.3354/meps10630

Padín, X. A., and others. 2010. Air-Sea CO_2 fluxes in the Atlantic as measured during boreal spring and autumn. Biogeosciences **7**: 1587–1606. doi:10.5194/bg-7-1587-2010

Paytan, A., K. R. M. Mackey, Y. Chena, I. D. Limac, S. C. Doneyc, N. Mahowaldd, R. Labiosae and A. F. Post. 2009. Toxicity of atmospheric aerosols on marine phytoplankton. Proc. Natl. Acad. Sci. USA **106**: 4601–4605. doi:10.1073/pnas.0811486106

Peñuelas, J., and others. 2013. Human-induced nitrogen-phosphorus imbalances alter natural and managed ecosystems across the globe. Nat. Commun. **4**: 2934. doi:10.1038/ncomms3934

Piccolo, M. C., and G. M. E. Perillo. 1999. Estuaries of Argentina: A review, p. 101–132. *In* G. M. E. Perillo, M. C. Piccolo, and M. Pino Quivira [eds.], Estuaries of South America: Their geomorphology and dynamics. Springer-Verlag.

Porra, R. J. 2002. The chequered history of the development and use of simultaneous equations for the accurate determination of chlorophylls *a* and *b*. Photosynth. Res. **73**: 149–156. doi:10.1023/A:1020470224740

Pulido-Villena, E., T. Wagener, and C. Guieu. 2008. Bacterial response to dust pulses in the western Mediterranean: Implications for carbon cycling in the oligotrophic ocean. Global Biogeochem. Cycles **22**: GB1020. doi:10.1029/2007GB003091

Raven, J. A. 1997. Phagotrophy in phototrophs. Limnol. Oceanogr. **42**: 198–205. doi:10.4319/lo.1997.42.1.0198

Regaudie-de-Gioux, A., and C. M. Duarte. 2013. Global patterns in oceanic planktonic metabolism. Limnol. Oceanogr. **58**: 977–986. doi:10.4319/lo.2013.58.3.0977

Ridame, C., J. Dekaezemacker, C. Guieu, S. Bonnet, S. L. Helguen, and F. Malien. 2014. Contrasted saharan dust events in LNLC environments: Impact on nutrient dynamics and primary production. Biogeosciences **11**: 4783–4800. doi:10.5194/bg-11-4783-2014

Roberts, B. J., and R. W. Howarth. 2006. Nutrient and light availability regulate the relative contribution of autotrophs and heterotrophs to respiration in freshwater pelagic ecosystems. Limnol. Oceanogr. **51**: 288–298. doi:10.4319/lo.2006.51.1.0288

Romero, S. I., A. R. Piola, M. Charo, and C. A. Eiras Garcia. 2006. Chlorophyll-a variability off Patagonia based on SeaWiFS data. J. Geophys. Res. **111**: C05021. doi:10.1029/2005JC003244

Strathmann, R. R. 1967. Estimating the organic carbon content of phytoplankton from cell volume or plasma volume. Limnol. Oceanogr. **12**: 411–418. doi:10.4319/lo.1967.12.3.0411

Strickland, J. D. H., and T. R. Parsons. 1972. A practical handbook of seawater analysis. Fish. Res. Board Can. Bull. **167**: 1–310. doi:10.1002/iroh.19700550118

Striebel, M., S. Bartholmé, R. Zernecke, C. Steinlein, F. Haupt, S. Diehl, and H. Stibor. 2009. Carbon sequestration and stoichiometry of motile and nonmotile green algae. Limnol. Oceanogr. **54**: 1746–1752. doi:10.4319/lo.2009.54.5.1746

Tanaka, T. Y., and M. Chiba. 2006. A numerical study of the contributions of dust source regions to the global dust budget. Glob. Planet. Change **52**: 88–104. doi:10.1016/j.gloplacha.2006.02.002

Teira, E., and others. 2016. Bacterioplankton responses to riverine and atmospheric inputs in a coastal upwelling system (Ría de Vigo, NW Spain). Mar. Ecol. Prog. Ser. **542**: 39–50. doi:10.3354/meps11565

Tsagaraki, T. M., and others. 2017. Atmospheric deposition effects on plankton Communities in the Eastern Mediterranean: A mesocosm experimental approach. Front. Mar. Sci. **4**: 210. doi:10.3389/fmars.2017.00210

Villafañe, V. E., and F. M. H. Reid. 1995. Métodos de microscopía para la cuantificación del fitoplancton, p. 169–185.

In K. Alveal, M. E. Ferrario, E. C. Oliveira, and E. Sar [eds.], Manual de métodos ficológicos. Universidad de Concepción.

Villafañe, V. E., S. D. Guendulain-García, F. Valadez, G. Rosiles-González, E. W. Helbling, and A. T. Banaszak. 2015. Antagonistic and synergistic responses to solar ultraviolet radiation and increased temperature of phytoplankton from cenotes (sink holes) of the Yucatán Peninsula, México. Freshw. Sci. **34**: 1282–1292. doi:10.1086/682051

Villafañe, V. E., M. J. Cabrerizo, G. S. Erzinger, P. Bermejo, S. M. Strauch, M. S. Valiñas, and E. Walter Helbling. 2017. Photosynthesis and growth of temperate and sub-tropical estuarine phytoplankton in a scenario of nutrient enrichment under solar ultraviolet radiation exposure. Estuaries Coast. **40**: 842–855. doi:10.1007/s12237-016-0176-z

Williamson, C. E., and others. 2014. Solar ultraviolet radiation in a changing climate. Nat. Clim. Chang. **4**: 434–441. doi:10.1038/nclimate2225

Zar, J. H. 1999. Biostatistical analysis, 4th ed. Prentice Hall.

Zubkov, M. V., M. A. Sleigh, G. A. Tarran, P. H. Burkill, and R. J. G. Leakey. 1998. Picoplanktonic community structure on an Atlantic transect from 50°N to 50°S. Deep-Sea Res. Part I **45**: 1339–1355. doi:10.1016/S0079-6611(00)00008-2

Zubkov, M. V., and P. H. Burkill. 2006. Syringe pumped high speed flow cytometry of oceanic phytoplankton. Cytometry A **69**: 1010–1019. doi:10.1002/cyto.a.20332

Zubkov, M. V., P. H. Burkill, and J. N. Topping. 2007. Flow cytometric enumeration of DNA-stained oceanic planktonic protists. J. Plankton Res. **29**: 79–86. doi:10.1093/plankt/fbl059

Acknowledgments

We are very grateful to P. Bermejo for nutrient analyses, to David Nesbitt for English-writing assistance, and to GES DISC scientists and associated NASA personnel for the production of the data used in this research effort. Comments and suggestions by Editor-in Chief Robert Howarth, associate Editor Heidi Sosik and two anonymous reviewers on a previous version of our manuscript are deeply acknowledged. We also thank Cooperativa Eléctrica y de Servicios de Rawson for building' infrastructure. This work was supported by Agencia Nacional de Promoción Científica y Tecnológica – ANPCyT (PICT 2012-0271 and PICT 2013-0208), Consejo Nacional de Investigaciones Científicas y Técnicas (PIP N° 112-201001-00228) and Ministerio de Economía y Competitividad (MEC) and Fondo Europeo de Desarrollo Regional (FEDER) (CGL2011-23681 and CGL2015-67682-R). PC and JMMS's visit to Estación de Fotobiología Playa Unión (EFPU) were supported by ANPCyT (PICT 2012-0271 and PICT 2013-0208). MJC was supported by a "Formación de Profesorado Universitario" Ph.D. grant of the Ministerio de Educación, Cultura y Deporte – MECD (FPU12/01243), two short-term placement grants at EFPU funded by MECD (EST13/0666) and Ceibiotic – UGR (call 2015), a postdoctoral contract 'Contrato Puente" funded by the Plan Propio of the University of Granada (FP7/2017) and by MEC-FEDER (CGL2015-67682-R), and Fundación Playa Unión. This work was in partial fulfilment of the Ph.D. thesis of MJC. This is contribution N° 170 of Estación de Fotobiología Playa Unión.

Conflict of Interest

None declared.

Submitted 23 August 2017
Revised 03 November 2017
Accepted 17 November 2017

Associate editor: Heidi Sosik